metals

MDPI

Article

Effectiveness of Thermal Annealing in Recovery of Tensile Properties of Compositionally Tailored PWR Model Steels Irradiated in LYRA-10

Mathilde Laot [1], Kiki Naziris [1], Theo Bakker [1], Elio D'Agata [2], Oliver Martin [2] and Murthy Kolluri [1,*]

[1] Nuclear Research & Consultancy Group (NRG), 1755 LE Petten, The Netherlands; laot@nrg.eu (M.L.); naziris@nrg.eu (K.N.); t.bakker@nrg.eu (T.B.)
[2] European Commission, Joint Research Centre (JRC), Directorate G—Nuclear Safety & Security, 1755 LE Petten, The Netherlands; elio.dagata@ec.europa.eu (E.D.); oliver.martin@ec.europa.eu (O.M.)
* Correspondence: kolluri@nrg.eu; Tel.: +31-224-568-418

Abstract: Understanding the mechanical behaviour of reactor pressure vessel (RPV) steels at high fluences has become an important topic in regard to Long-Term Operations (LTO) of existing nuclear power plants (NPP). The effectiveness of thermal annealing treatments to recover the mechanical properties of compositionally tailored pressurised water reactor (PWR) model steels irradiated to high neutron fluences, up to 1.22×10^{20} n·cm^{-2}, is analysed in this study. Tensile testing of four different PWR RPV steels was performed after irradiation and subsequent recovery annealing treatment at 450 °C for 40 h. Irradiation-induced hardening and the effectiveness of recovery thermal annealing have been assessed by comparing the strength and ductility properties of irradiated and irradiated and subsequently annealed samples with unirradiated reference samples for all four model steel. The annealing treatment resulted in a significant recovery of the yield strength (~75–89%) and the ultimate tensile strength (~78–96%) of all four PWR model steels. This study proves that substantial irradiation-induced hardening (up to ~389 MPa) observed in steels containing high Ni and Mn contents can still be recovered using the thermal annealing treatment. No influence of annealing on ductility properties has been observed for all four model steels. Microscopy analyses of these steels to understand the underlying irradiation damage and recovery mechanisms are planned for the near future.

Keywords: long-term operation; RPV embrittlement; LYRA-10 irradiation; thermal annealing; recovery; PWR RPV steels

Citation: Laot, M.; Naziris, K.; Bakker, T.; D'Agata, E.; Martin, O.; Kolluri, M. Effectiveness of Thermal Annealing in Recovery of Tensile Properties of Compositionally Tailored PWR Model Steels Irradiated in LYRA-10. *Metals* **2022**, *12*, 904. https://doi.org/10.3390/met12060904

Academic Editors: Pasquale Cavaliere and Ferenc Gillemot

Received: 28 March 2022
Accepted: 23 May 2022
Published: 25 May 2022

1. Introduction

For the majority of currently operating nuclear power plants (NPP), long-term operation (LTO) is either under consideration or already a reality. A critical component for ensuring the safe lifetime extension of an NPP beyond its original design life is the reactor pressure vessel (RPV). The structural integrity of the RPV must be ensured for the entire lifetime of the reactor under normal operational conditions, including reactor transients such as reactor start-up and -shutdown, and possible off-normal operational conditions (e.g., emergency core cooling and resulting pressurised thermal shock). The level of RPV ductility is assessed through surveillance programmes of the NPPs. Exposure of the RPV to fast neutron irradiation during operation causes embrittlement of the RPV with associated changes in mechanical properties (increase in hardening, reduction in ductility). The formation of irradiation-induced matrix defects (MDs) and solute clusters (SCs) cause irradiation hardening as they act as obstacles to the dislocation motion. In addition, irradiation-induced segregation of impurities such as P and S, although not causing any hardening, contributes to the embrittlement. Both hardening and non-hardening features result in an increase in the ductile-to-brittle transition temperature (DBTT) of RPV steels.

Recovery annealing is generally considered a last resort for the mitigation of the irradiation-induced embrittlement of RPV steels [1]. Annealing can, to some degree, recover the transition temperature shift of the irradiated beltline region and recover the upper shelf energy. This procedure can therefore be used to extend the lifetime of RPV to support the LTO of NPPs [2]. Thermal annealing in RPV steels differs from the traditional metallurgical thermal annealing of carbon steels at temperatures up to 1000 °C, but it is a localised heat treatment at lower temperatures (typically between 340 °C and 500 °C) and for a long holding time (up to ~150 h) [1]. A number of studies have demonstrated the partial or even full recovery of the mechanical properties of irradiated RPV steels (both low- and high-Cu content) after applying recovery annealing treatment [1–5].

Initially, recovery annealing treatments of RPVs of Water-Water Energetic Reactor (VVER)-type reactors were developed for VVER-440 RPV welds with high impurity content of Cu and P. Several RPVs of VVER-440 reactors have been successfully annealed by means of thermal treatment at the optimised temperature–time regime (475 °C, 100 h) [6]. Annealing of VVER-440 RPV steels, or Cu-rich RPV steels in general, leads to partial dissolution of the irradiation-induced Cu-rich SCs and the coarsening of the remaining SCs, while the mechanical properties experience recovery (e.g., [2,7,8]).

PWR RPV steels have a much lower Cu-content compared to VVER-440 RPV steels. In these low-Cu RPV steels, irradiation-induced embrittlement cannot be solely described in terms of Cu-rich precipitates and matrix damage [8]. Instead, beginning in the early 1990s, the formation of Ni-Mn-Si-rich clusters in low-Cu RPV steels was proposed as the cause for their irradiation-induced embrittlement [9]. In general, the dissolution of the Ni-Mn-Si-rich irradiation-induced clusters starts at ~400 °C [8,10–12]. The effectiveness of recovery annealing increases with temperature [11,13]. A clear correlation between the dissolution of Ni-Mn-Si-rich clusters and recovery of the mechanical properties of the RPV materials was reported in the literature [3,8,14]. Unlike the Cu-rich precipitates, which partially dissolve and partially coarsen during recovery annealing treatment, Ni-Mn-Si-rich clusters dissolve without coarsening. It is assumed that Mn plays an important role in the dissolution mechanism of the clusters [8]. Mn is known to couple strongly with point defects and therefore the diffusion of Mn away from the clusters could be related to the expulsion of point defects from the clusters upon annealing [8].

Currently, not many data on the recovery of low-Cu RPV steels irradiated to high fluences are available [15,16]. Besides that, there is evidence in the literature for accelerated embrittlement at high neutron fluences, and the extent of recovery that can be achieved with thermal annealing in such cases is not well investigated. In this study, the effectiveness of thermal annealing to recover tensile properties of highly irradiated compositionally tailored PWR RPV model steels is presented and discussed. The examined model steels with systematic variations in Ni and Mn contents were part of the joint NRG-JRC irradiation experiment, LYRA-10. The LYRA-10 specimens were irradiated in the High Flux Reactor (HFR) in Petten to fluences resembling reactor operation times of 60–80 years at typical PWR/VVER operating temperatures of around 286 °C.

2. Materials and Methods

2.1. Materials

The chemical composition of the four PWR RPV model steels studied in this paper, hereafter referred to as model steels K, L, M, and N, is shown in Table 1. Model steels K, L and M have increasing Ni content with almost identical Mn content, while mode steel N has almost the same Ni content as model steel M, but a much higher Mn content. The systematic variation in Ni and Mn content allowed us to investigate the individual and synergetic effects of Ni and Mn on the embrittlement of PWR RPV steels at high fluences [17]. In this paper, the effectiveness of thermal annealing in recovering tensile properties of these compositionally tailored PWR model steels is studied.

Table 1. Chemical composition of the four PWR model steels investigated in this research (in mass %).

Model Steel Grade	C	Si	Mn	Cr	Ni	Mo	V	Cu	S	P
K	0.17	0.35	0.78	0.10	0.58	0.64	-	0.07	0.005	0.009
L	0.18	0.35	0.77	0.08	0.96	0.63	-	0.05	0.005	0.010
M	0.16	0.37	0.74	0.09	1.90	0.61	-	0.05	0.005	0.010
N	0.16	0.33	1.27	0.07	1.97	0.63	-	0.06	0.005	0.010

The nominal base compositions of the 4 model steel types were derived from the typical Western PWR RPV steel ASME SA508 Cl.2, 1989. The model steels were produced in an open induction furnace with a special iron charge containing secondary elements. Cast iron was added to the charges to increase the carbon content to the required level. The alloying elements (Ni and Mn) were doped to the charges in the form of master alloys. The desired levels of the impurity elements Cu, P, and S were achieved by adding metallic Cu, an Fe-P compound (with 25% of P), and an Fe-S compound (with 36.4% of S), respectively. Each melt was cast into an ingot weighing 25 kg each. All the ingots were heated for 4 h at 800 °C and then forged into bars with a 50 × 50 mm cross-section. Forging was carried out at temperatures ranging from 900 to 1200 °C. The sink head of each ingot was removed after forging. Subsequently, the forged bars were hot-rolled into plates approximately 8 mm thick and 200–210 mm wide. Rolling was performed at 1180 °C with preheating of about 2 h. The finished plates were cut into pieces 600–700 mm in length.

A series of heat treatments were applied to 8-mm-thick plates with the aim to achieve the matching yield strength levels (=550 ± 30 MPa) and a similar bainite-martensite microstructure for all model steels independent of their chemical composition. The yield stress was controlled by hardness measurement. In the first stage, the plates were tempered for 10 h at 640 °C. In the second stage, hardening and tempering treatments were applied to achieve the target strength levels. The regimes involve a hardening stage of heating the model steel plates from 600 °C to 900 °C (for steels L, M, N) and 600 °C to 940 °C (for steel K), the maintenance of the plate temperature at that level for 20 min, and subsequent cooling in water. The hardening stages were followed by a tempering stage involving heating of the model steel plates for several hours (K & L = 12 h, M = 10 h, N = 20 h) at 640 °C in air until the desired strength level was achieved for all the model steels [18].

2.2. LYRA-10 Irradiation

LYRA-10 is a joint irradiation experiment carried out by NRG and JRC at the HFR in Petten (Figure 1). The total irradiation lasted for 16 HFR cycles (~467 full-power days at a nominal reactor power level of 45 MW) and a nominal fast neutron fluence (E > 1 MeV) of 1.11 × 10^{20} n·cm^{-2} at an average temperature of 286 °C. Figure 2 shows the fluence profiles (for the total irradiation duration) along the length of the irradiation capsule at all four corners. The experiment was rotated two times by 180° each to achieve a uniform fluence distribution for all specimens. However, due to the LYRA-10's position in the layout of the HFR's core, corner 1–2 received a higher dose. Table 2 shows the nominal fast fluence (E > 1 MeV) values, including the minimum, maximum, and standard deviation, which the tensile specimens made of the 4 model steel types have received. Given that the design operating lifetime fluence (E > 1 MeV) for 32 effective full-power years (EPFY) of a typical PWR RPV is 4 × 10^{19} n·cm^{-2}, the nominal fast fluence (E > 1 MeV) of 1.11 × 10^{20} n·cm^{-2} received by the LYRA-10 specimens investigated here corresponds to ~89 EPFY. The nominal dpa value is 0.18. The nominal flux (E > 1 MeV) value is ~2.75 × 10^{12} n·cm^{-2}·s^{-1}, which is slightly more than two orders of magnitude higher than the design flux value of a typical PWR RPV.

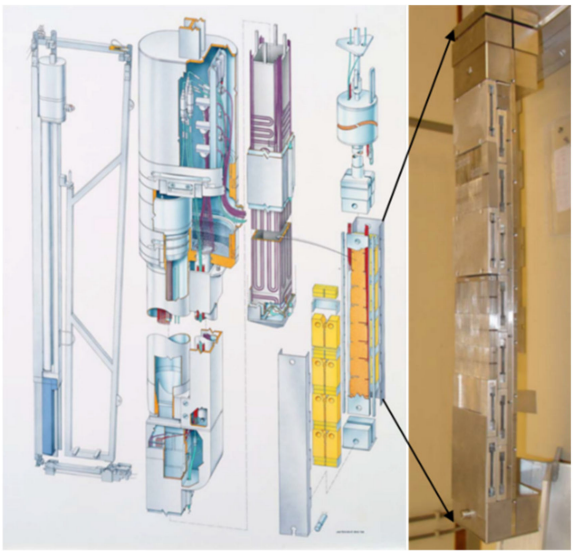

Figure 1. Schematic showing the LYRA irradiation facility at HFR Petten and the LYRA-10 capsule loaded with RPV steel specimens.

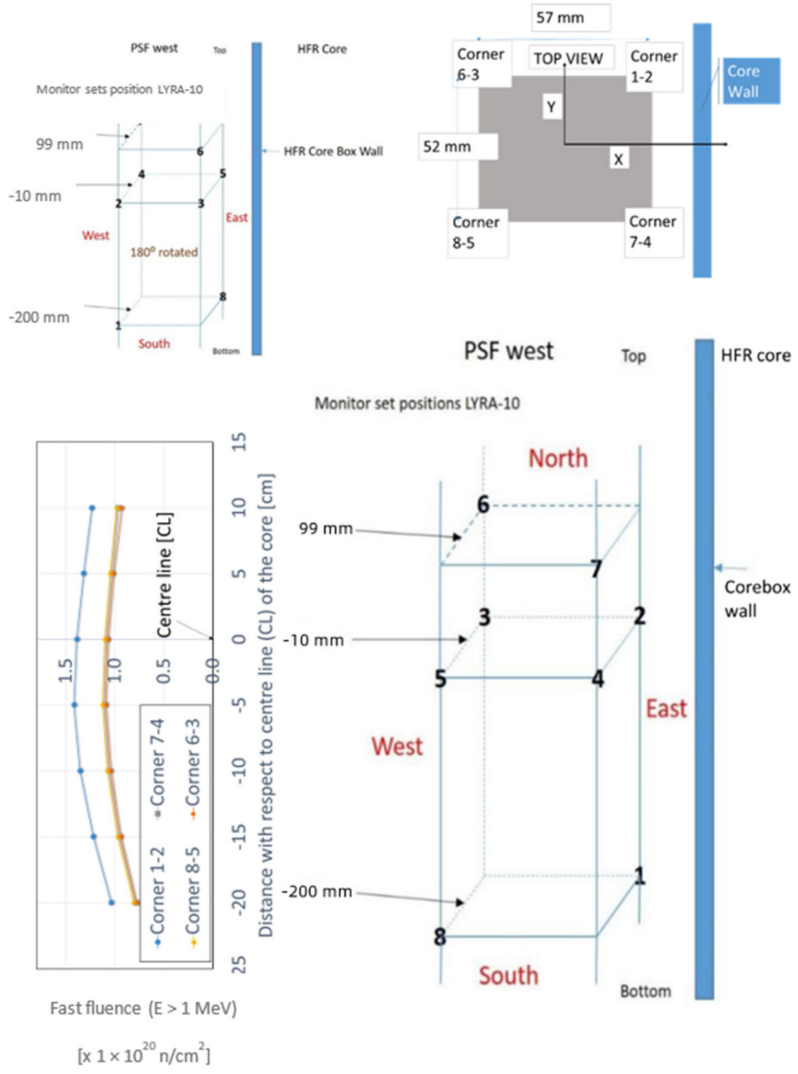

Figure 2. The fluence profiles (for the total irradiation duration) along the length of the irradiation capsule at four corners.

Table 2. Nominal fast fluence values of the tensile specimens of the four PWR RPV model steel types irradiated in LYRA-10.

Steel Grade	Nominal Fast Fluence ($\times 10^{20}$ n·cm^{-2})			
	Tensile Specimens			
	Mean	Min.	Max.	Std. Dev.
K	1.18	1.13	1.22	0.035
L	1.05	1.02	1.09	0.026
M	1.06	0.97	1.15	0.081
N	1.09	1.02	1.17	0.053

LYRA-10 included, in total, more than 600 specimens of different types (e.g., tensile, Charpy, mini-Charpy, and microscopy) of RPV model steels representative of VVER-1000 and PWR RPV steels with systematic variations in Ni and Mn content and, to a smaller extent, Si content. A large PIE testing campaign on the LYRA-10 specimens is currently ongoing within the STRUMAT-LTO project, which is an international collaboration project funded by EURATOM (Grant agreement no. 945272) and involving 18 organisations. The research presented in this paper has been jointly performed by NRG and JRC as part of the STRUMAT-LTO in-kind pilot project before the start of the EURATOM-funded STRUMAT-LTO project. This paper addresses the extent of recovery of highly irradiated compositionally tailored PWR model steels, after recovery annealing treatment for 40 h at 450 °C.

2.3. Test Matrix

A mechanical testing campaign was conducted including several tensile specimens for each model steel in unirradiated, irradiated, and irradiated and annealed states. For the irradiated specimens, the tensile properties were measured at room temperature. For each grade, two irradiated specimens were thermally annealed for 40 h at 450 °C prior to testing, to study the effectiveness of annealing treatment in recovering the tensile properties. Due to the limited number of available specimens, only one tensile specimen per model steel was tested in unirradiated conditions at room temperature. Table 3 shows the test matrix of the study and Figure 3 shows the specimen geometry. Tensile testing of all specimens was performed at NRG's hot cell laboratories (HCL).

Table 3. Test matrix of unirradiated, irradiated, and post-irradiation annealed specimens.

Test Type	Steel Grade	Number of Specimens Tested		
		Unirradiated (Tested at Room Temperature)	Irradiated (Tested at Room Temperature)	Irradiated, Annealed at 450 °C for 40 h (Tested at Room Temperature)
Tensile	**K**	1	2	2
	L	1	2	2
	M	1	2	2
	N	1	2	2

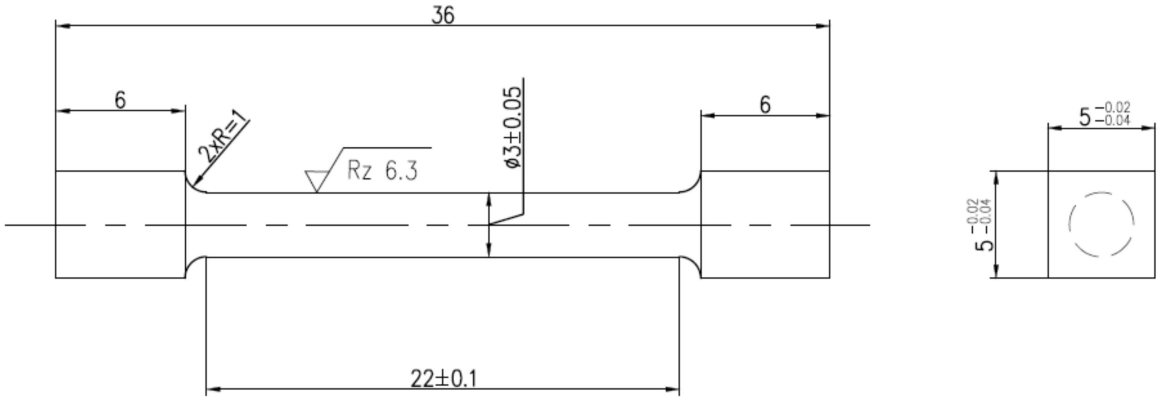

Figure 3. Geometry of the tensile specimens.

2.4. Post-Irradiation Annealing Treatments

For each model steel, two irradiated specimens were annealed in air at 450 °C for 40 h using an electrical SEVERN furnace (model number SF835). Afterwards, furnace cooling was applied.

2.5. Tensile Tests

The tensile tests were performed in accordance with ASTM E8M [19]. All tensile tests were performed at room temperature (25 ± 2 °C) using an Instron servo-mechanical test machine equipped with a 10 kN load cell. The tensile test machine is located in the G3 hot cell of the NRG Hot Cell Laboratories. The tests were executed at a constant cross-head velocity resulting in an initial strain rate of 5×10^{-4} s^{-1}. After the test, the data were analysed in accordance with ASTM E8M. The following properties were determined from the recorded engineering stress–strain curves:

- 0.2% offset yield stress (0.2% YS).
- Ultimate tensile strength (UTS).
- % uniform (plastic) elongation (%UE).
- % total elongation (%TE), i.e., elongation at fracture.

Note that no external extensometer was used during tensile testing, and hence, the uniform and total elongation values are measured from the cross-head displacement of the Instron machine.

3. Results

Tensile stress–strain curves of all four model steel types in unirradiated (reference), irradiated, and irradiated–annealed conditions are shown in Figure 4a–d. A comparison of the tensile properties (YS, UTS, %UE, and %TE) of all four model steel types in reference, irradiated, and irradiated–annealed conditions are shown in Figure 5a–d. The presented tensile properties in Figure 5 are the average values obtained from the two tested specimens for each condition, except for the unirradiated state for which only one specimen per model steel was tested at room temperature.

The irradiation-induced embrittlement of the K, L, M, and N model steels has been extensively presented and discussed by Kolluri et al. [17]. All four model steel types experience significant irradiation-induced hardening while the observed changes in ductility properties are minimal. From the irradiation hardening (ΔYS and ΔUTS) data plotted in Figure 6, two notable observations can be made. The role of the Ni-content of RPV steels and the synergetic influence of Ni and Mn on the irradiation hardening at high neutron fluence values. The increase of ~1% Ni-content in grade M with respect to grade L led to a significant increase in ΔYS (from 146 MPa to 309 MPa), which demonstrates that the Ni-content increases the sensitivity of RPV steels to irradiation hardening. The additional increase in irradiation hardening observed for steel grade N compared to grade

M emphasises the importance of the Mn-content in the radiation hardening mechanism in case of a high Ni-content.

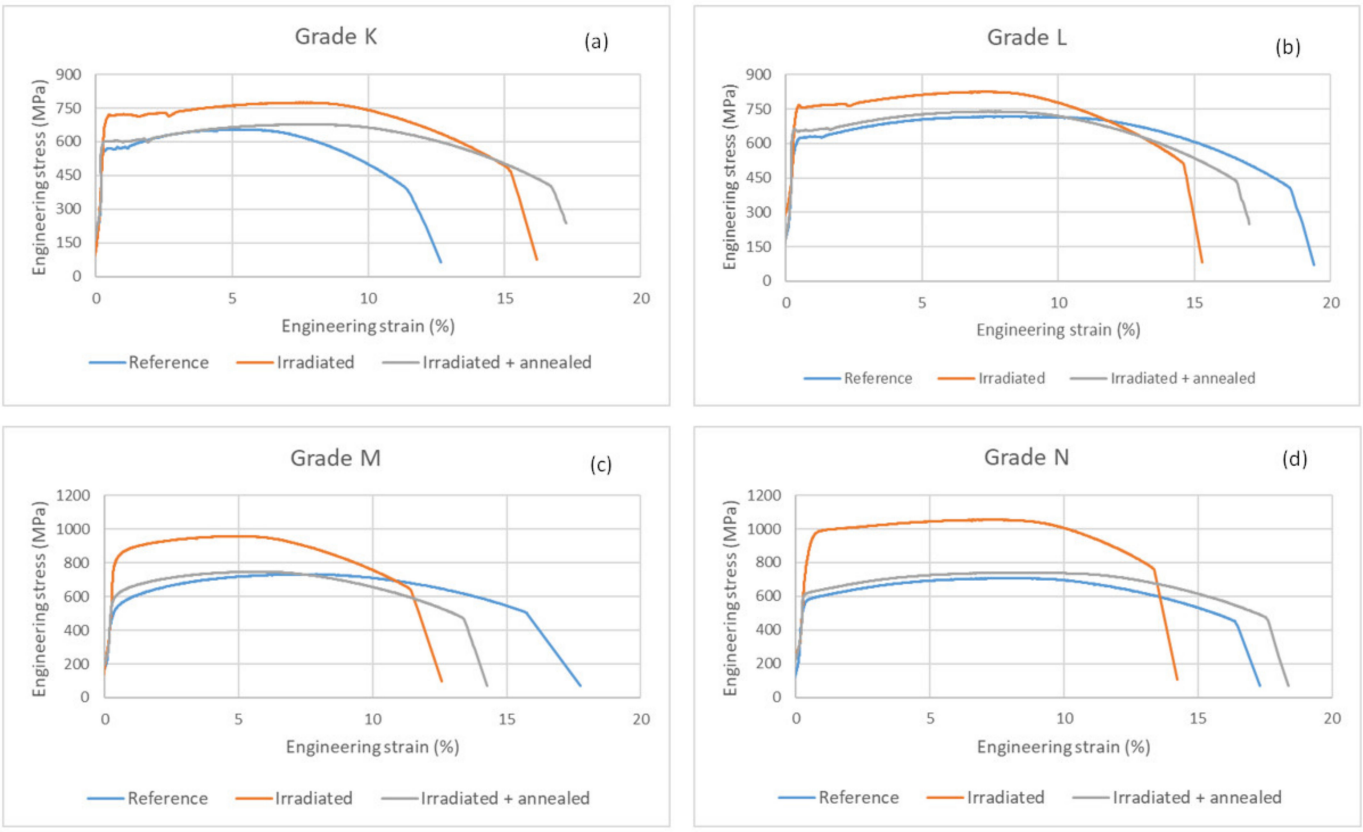

Figure 4. Comparison of tensile stress–strain curves in reference, irradiated, and post-irradiation annealed states for (**a**) model steel grade K, (**b**) model steel grade L, (**c**) model steel grade M and (**d**) model steel grade N.

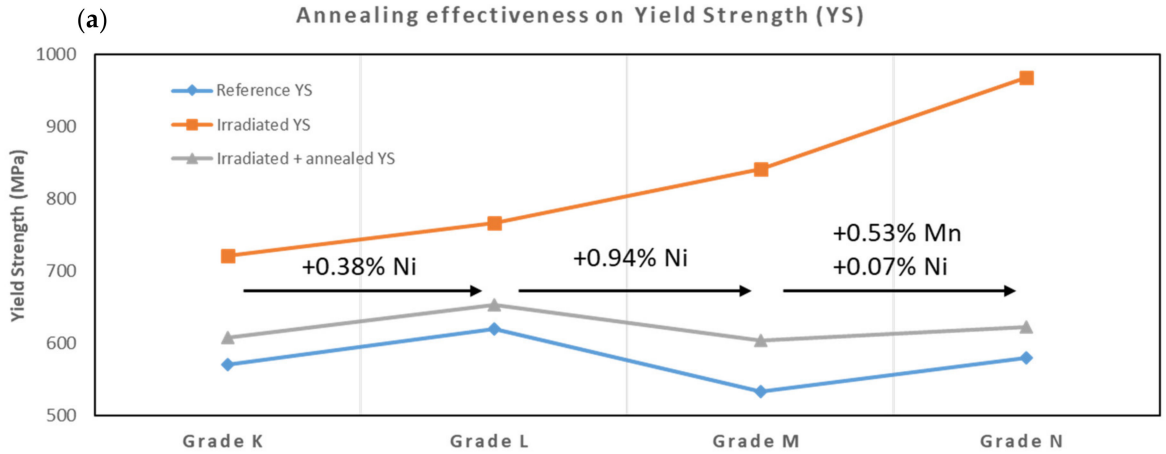

Figure 5. *Cont.*

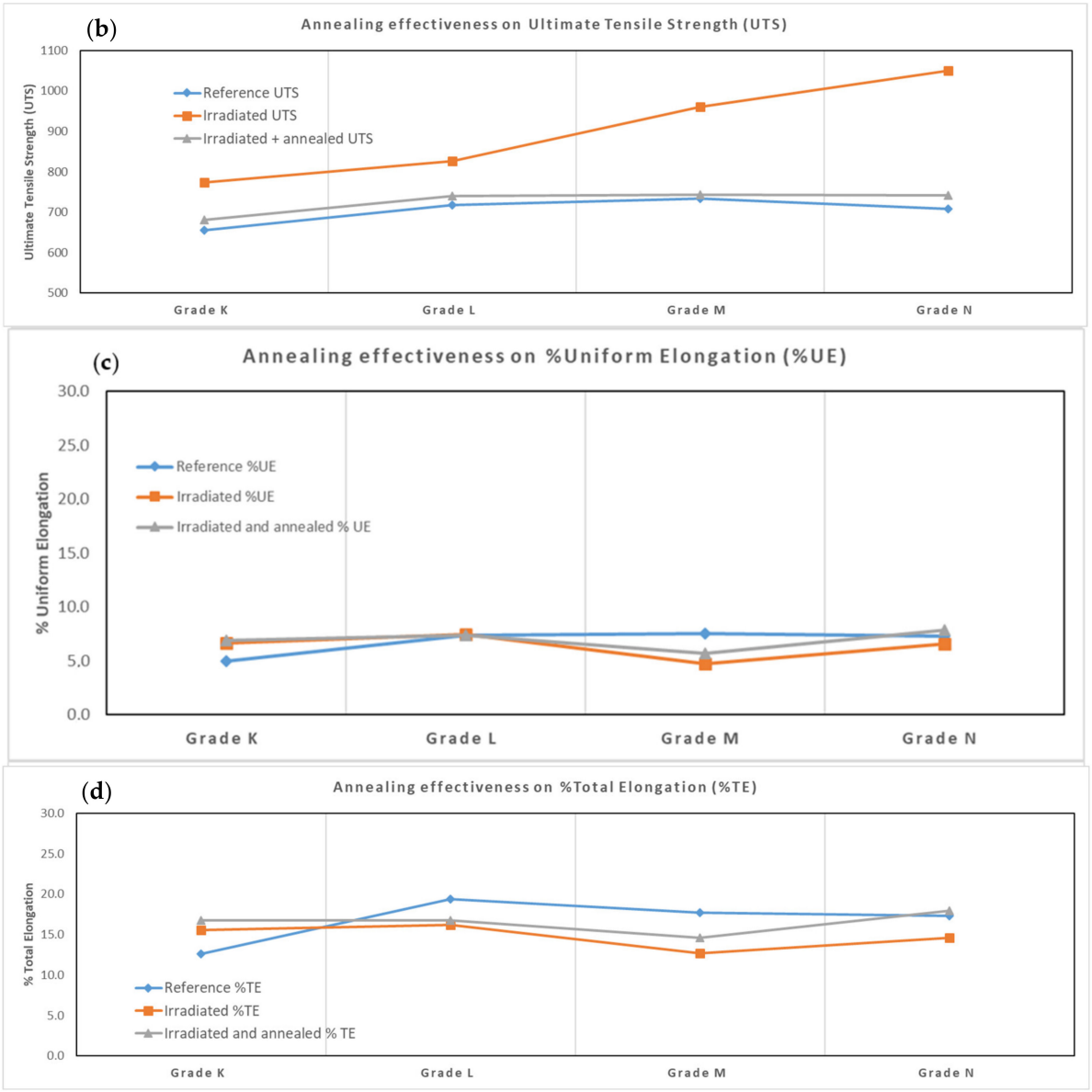

Figure 5. Comparison of (**a**) YS, (**b**) UTS, (**c**) %UE, and (**d**) %TE properties of the four model steel types in unirradiated, irradiated, and irradiated-annealed conditions.

Figure 7 shows the effectiveness of annealing for all four model steel types. The $\%YS_{recovery}$ and $\%UTS_{recovery}$ refer to the recovery in YS and UTS, respectively, after annealing, as given by the ratio below:

$$\%YS_{recovery} = \frac{YS_{irradiated} - YS_{annealed}}{YS_{irradiated} - YS_{reference}} * 100 \quad (1)$$

This ratio provides the effectiveness of annealing with respect to irradiation hardening. It must be noted that the effect of the different fluences received by each grade during irradiation is neglected in comparison to the effect of chemical composition.

It can be seen that the annealing treatment led to a significant recovery of tensile properties for all four model steel types. The relative recovery of the yield strength (YS) is slightly lower than the recovery of the ultimate tensile strength (UTS), except for grade M, which shows a significant difference between YS and UTS recovery. The recovery of YS for grades K, L, and M are similar while grade N, with a higher content of Mn (1.27 wt.% compared to 0.74–0.78 wt.%), shows a higher recovery of YS. Model steels with

high Ni content (grades M and N) show a higher recovery of UTS than with lower Ni content (grades K and L). Recovery of uniform elongation and total elongation is found to be negligible. Only a slight change in ductility was observed after irradiation, and after annealing the elongations (%TE and %UE), values are close to irradiated values. Only Grade N with a higher Mn content shows a slight recovery of its total elongation.

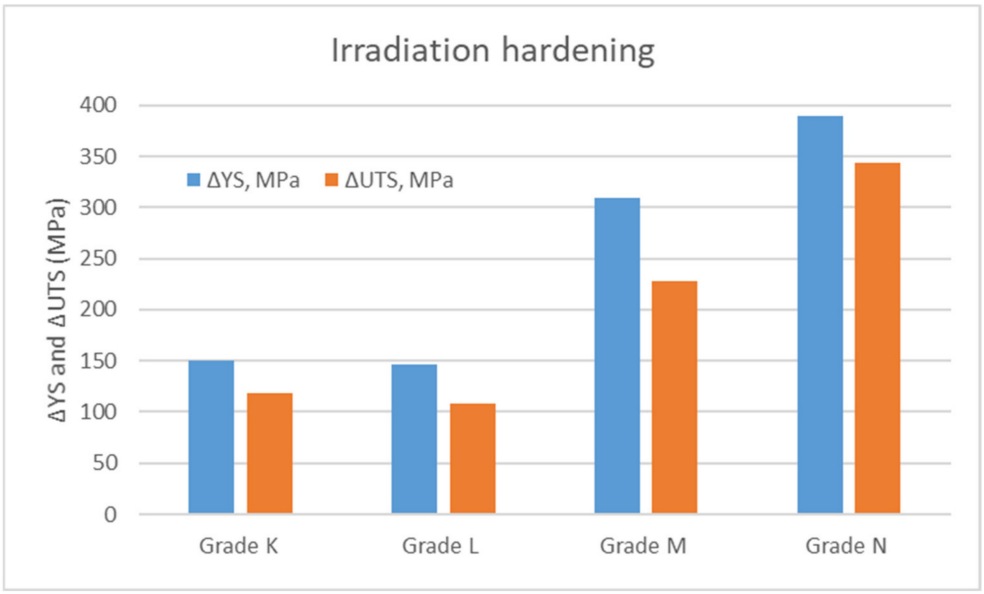

Figure 6. Comparison of irradiation hardening of all four model steel grades.

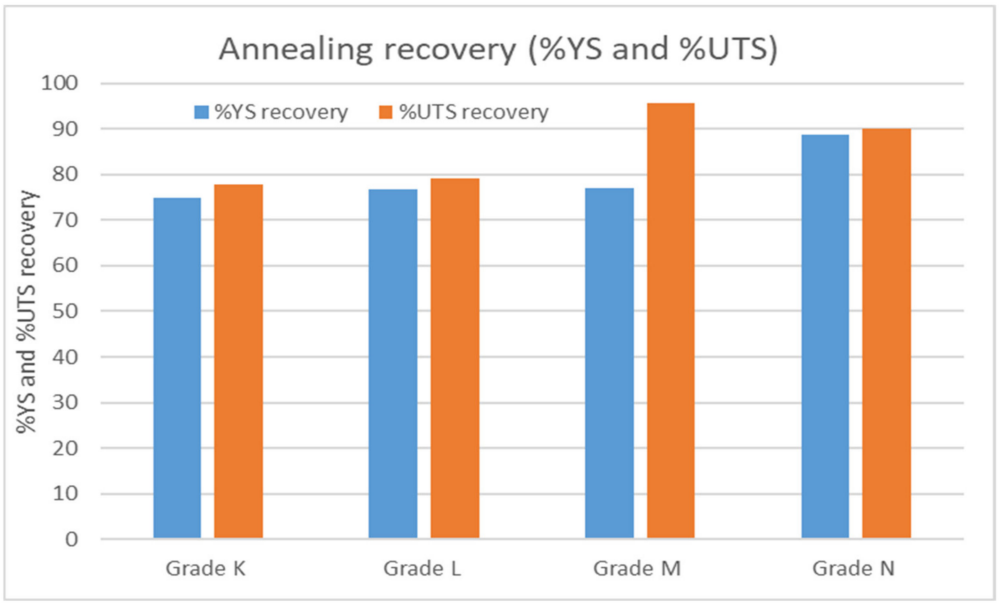

Figure 7. Comparison of tensile properties recovery after annealing of four irradiated model steel types.

4. Discussion

It is well known that upon neutron irradiation, Ni-Mn-Si-rich clusters and matrix defects develop and grow or increase in number in low-Cu RPV steels. These irradiation-induced features act as obstacles to dislocation movement causing hardening and upward shifts in DBTT. As mentioned above, the highest hardening was found in the model steel with the highest Ni and Mn content (model steel N). The difference in the level of irradiation-induced hardening between model steels M and N suggests that Mn plays an important

role in the hardening mechanism in PWR RPV steels. Irradiation hardening of Fe-Mn binary alloys studied by Yabuuchi et al. [20] showed that irradiation hardening increases as a function of Mn-content, which is consistent with the results of this study. In addition, atom probe field microscopy results of irradiated low-Cu RPV steels presented in [17] show that the majority of irradiation-induced clusters are Mn-initiated.

All four investigated RPV model steels show significant recovery of their strength properties after recovery annealing treatment. This recovery is believed to be related to the (partial) dissolution of the radiation-induced clusters and the annihilation of matrix defects. The dissolution of the radiation-induced Ni-Mn-Si-rich precipitates in low-Cu RPV steels upon annealing has been already demonstrated in various studies (e.g., [20–22]). For VVER-1000 RPV welds, the basic annealing mode for recovering their mechanical properties is at 565 °C for 100 h [3,23]. TEM analyses by Gurovich et al. [22] showed that annealing at a lower temperature (i.e., 400 °C) already allows for partial dissolution of the irradiation-induced features and the recovery of mechanical properties of VVER structural materials for fast neutron fluence values between 0.25 and 0.5 $\times$ 10^{20} cm^{-2}. Similarly, Miller et al. [23] observed the dissolution of irradiation-induced Ni-, Mn-, and Si- enriched nanoclusters (for fast neutron irradiation fluences between 0.25 and 1.49 $\times$ 10^{20} cm^{-2}) after annealing at 450 °C for 24 h, whereas after annealing at 450 °C for only 2 h, the nanoclusters were still present.

Unlike Cu-rich clusters, which form upon neutron irradiation in high-Cu RPV steels via a vacancy-driven mechanism, Ni-Mn-Si-rich clusters are assumed to nucleate via a self-interstitial-driven mechanism [3]. Ngayam-Happy et al. [24] showed that even in the absence of Cu, thermodynamic-kinetic models predict the formation of Mn-Ni phases at low nucleation rates and high incubation fluences. For this reason, they are called "late-blooming phases" and can lead to a substantial increase in the embrittlement rate after approximately 40 to 60 years of reactor operation in steels with high Ni and high Mn content.

The fluence values that the specimens in this study received resemble more than 60 years of reactor operation (nominal fast fluence values of 1.05–1.22 $\times$ 10^{20} cm^{-2}). The significant recovery of the strength properties of all examined model steels after only 40 h of annealing at the relatively modest temperature of 450 °C indicates almost full dissolution of irradiation-induced Ni-Mn-Si-rich clusters and matrix defects. Moreover, the recovery of strength properties indicates that no, or only insignificant, thermodynamically stable phases are formed due to irradiation to high neutron fluences. It should be noted that slight differences exist in the level of recovery of YS and UTS between the four model steel types. The lower recovery in YS of grade M could indicate a delay in the yield point phenomenon, likely due to the presence of some residual irradiation defects offering resistance to the dislocation motion. The residual hardening still present in all four model steel types after annealing could be related to the chosen annealing treatment. Annealing at 450 °C for the relatively short period of 40 h could be insufficient to fully dissolve the Ni-Mn-Si-rich clusters. Annealing temperatures [25] and holding times are known to affect the extent of DBTT recovery of irradiated RPV steels.

Mn content could be the cause of the slightly lower recovery of model steels K, L, and M observed compared to model steel N. The important role of Mn in the dissolution of the Ni-Mn-Si-rich clusters has been discussed by Styman et al. [8]. The dissolution of the clusters formed during irradiation could be driven by the expulsion of point defects since Mn is known to couple strongly with point defects. In addition, Yabuuchi et al. [20] state that Mn increases the number of dislocation loops, which contribute to the irradiation hardening. Mn atoms behave as nuclei for the loops by trapping the interstitial atoms and interstitial clusters generated by cascades. It is well known that dislocation loops formed due to neutron irradiation tend to disappear upon annealing [3,21] and this could explain the relatively high recovery of UTS model steel N.

Planned microstructural analyses, as part of the EURATOM-funded STRUMAT-LTO project, are expected to confirm the above theories.

5. Conclusions

The effectiveness of annealing four different PWR RPV model steel types at 450 °C for 40 h has been investigated. The annealing resulted in a significant recovery of the strength properties (yield stress and ultimate tensile strength) for all four model steel types towards values of their unirradiated condition. The chemical composition of the model steels showed some influence on the recovery process during annealing. Model steels with high Ni and Mn content showed slightly higher recovery than steels with lower Ni and Mn content. TEM analyses are planned for the near future to further investigate the effect of Ni and Mn content. This behavior could be linked to the catalytic role of Mn in the dissolution mechanisms of irradiation-induced Ni-Mn-Si-rich clusters during annealing as indicated in several publications. Microscopy investigations of the four model steel types are intended to further elaborate our understanding of irradiation hardening and recovery mechanisms.

Author Contributions: Conceptualisation, M.K.; methodology, M.K. and O.M.; formal analysis, M.L. and K.N.; investigation, T.B.; data curation, M.L. and K.N.; writing—original draft preparation, M.L. and K.N.; writing—review and editing, M.K., E.D. and O.M.; visualisation, M.L.; supervision, M.K.; project administration, M.K.; resources, M.K., E.D. and O.M.; funding acquisition, M.K. All authors have read and agreed to the published version of the manuscript.

Funding: The research reported in the project is performed within the framework of the STRUMAT-LTO project. This project has received funding from the Euratom research and training programme 2019–2020 under grant agreement n° 945272. The work performed at NRG is co-funded by the Dutch Ministry of Economic Affairs (EZS).

Data Availability Statement: Data are contained within the article.

Conflicts of Interest: The authors declare no conflict of interest. The funders had no role in the design of the study; in the collection, analyses, or interpretation of data; in the writing of the manuscript, or in the decision to publish the results.

Export Control Note: The content within this document is classified with the code EU DuC = X. EU DuC represents the European dual use code.

Nomenclature

%TE	Total Elongation
%UE	Uniform Elongation
ASME	American Society of Mechanical Engineers
ASTM	American Society for Testing and Materials
DBTT	Ductile-Brittle Transition Temperature
HFR	High Flux Reactor
LTO	Long-Term Operation
MD	Matrix Defects
NPP	Nuclear Power Plant
PWR	Pressurized Water Reactor
RPV	Reactor Pressure Vessel
SC	Solute Clusters
UTS	Ultimate Tensile Strength
VVER	Water-Water Energetic Reactor
YS	Yield strength
ΔUTS	Change in UTS between annealed and reference condition
ΔYS	Change in YS between annealed and reference condition

References

1. Server, W.; Sokolov, M. Thermal Annealing of PRV Is a Needed Mitigation Option. In Proceedings of the Degradation of Primary Componenets of Pressurized Water Cooled Nuclear Reactors: Current Issues and Future Challenges, IAEA, Vienna, Austria, 5–8 November 2013.
2. Miller, M.; Nanstad, R.; Sokolov, M.; Russell, K. The effects of irradiation, annealing and reirradiation on RPV steels. *J. Nucl. Mater.* **2006**, *351*, 216–222. [CrossRef]

3. Gurovich, B.; Kuleshova, E.; Shtrombakh, Y.; Fedotova, S.; Erak, D.; Zhurko, D. Evolution of microstructure and mechanical properties of VVER-1000 RPV steels under re-irradiation. *J. Nucl. Mater.* **2015**, *456*, 373–381. [CrossRef]
4. Miller, M.; Russell, K. Atom probe characterization of copper solubility in the Midland weld after neutron irradiation and thermal annealing. *J. Nucl. Mater.* **1997**, *250*, 223–228. [CrossRef]
5. Pareige, P.; Radiguet, B.; Suvorov, A.; Kozodaev, M.; Krasikov, E.; Zabusov, O.; Massoud, J.P. Three-dimensional atom probe study of irradiated, annealed and re-irradiated VVER 440 weld metals. *Surf. Interface Anal.* **2004**, *5*, 581–584. [CrossRef]
6. Kryukov, A.; Debarberis, L.; Ballesteros, A.; Krsjak, V.; Burcl, R.; Rogozhkin, S.; Nikitin, A.; Aleev, A.; Zaluzhnyi, A.; Grafutin, V.; et al. Integrated analysis of WWER-440 RPV weld re-embrittlement after annealing. *J. Nucl. Mater.* **2012**, *429*, 190–200. [CrossRef]
7. Naziris, N.; Kolluri, M.; Bakker, T.; Hageman, S.; Petrosyan, V.; Sevikyan, G. Mechanical properties and microstructure of VVER 440 RPV steels irradiated to extremely high fluences and the effect of recovery annealing. *J. Nucl. Mater.* **2021**, *551*, 152951. [CrossRef]
8. Styman, P.; Hyde, J.; Parfitt, D.; Wilford, K.; Burke, M.G.; English, C.; Efsing, P. Post-irradiation annealing of Ni–Mn–Si-enriched clusters in a neutron-irradiated RPV steel weld using Atom Probe Tomography. *J. Nucl. Mater.* **2015**, *459*, 127–134. [CrossRef]
9. Odette, G.R. Radiation induced microstructural evolution in reactoe pressure vessel steels. In *Material Research Society Symposium Proceedings*; Robertson, I.M., Rehn, L.E., Zinkle, S.J., Phythian, W.J., Eds.; MRS: Boston, MA, USA, 1995.
10. Odette, G.R.; Nanstad, R.K. Predictive reactor pressure vessel steel irradiation embrittlement models: Issues and opportunities. *JOM* **2009**, *61*, 17–23. [CrossRef]
11. Kryukov, A.; Nikolaev, Y. The properties of WWER-1000 type materials obtained on the basis of a surveillance program. *Nucl. Eng. Des.* **2000**, *195*, 143–148. [CrossRef]
12. Guionnet, C.; Houssin, B.; Brasseur, D.; Lefort, A.; Groß, D.; Perdreau, R. Radiation Embrittlement of PWR Reactor Vessel Weld Metals: Nickel and Copper Synergism Effects. *Eff. Radiat. Mater.* **1982**, 392–411.
13. Bergner, F.; Ulbricht, A.; Lindner, P.; Keiderling, U.; Malerba, L. Post-irradiation annealing behavior of neutron-irradiated FeCu, FeMnNi and FeMnNiCu model alloys investigated by means of small-angle neutron scattering. *J. Nucl. Mater.* **2014**, *454*, 22–27. [CrossRef]
14. Kuleshova, E.; Gurovich, B.; Shtrombakh, Y.; Erak, D.; Lavrenchuk, O. Comparison of microstructural features of radiation embrittlement of VVER-440 and VVER-1000 reactor pressure vessel steels. *J. Nucl. Mater.* **2002**, *300*, 127–140. [CrossRef]
15. Server, W.L.; Hardin, T.C.; Hall, J.B.; Nanstad, R.K. U.S. High Fluence Power Reactor Surveillance Data—Past and Future. *J. Press. Vessel. Technol.* **2014**, *2*, 021603. [CrossRef]
16. Server, W.E.A. Need for High Fluence RPV Reactor Surveillance Data for Long Term Operation. In Proceedings of the IAEA Technical Meeting on Degradation of Primary Components of Pressurized Water Cooled Nuclear Reactors: Current Issues and Future Challenges, Vienna, Austria, 5–8 November 2013.
17. Kolluri, M.; Pierick, P.T.; Bakker, T.; Straathof, B.T.; Magielsen, A.J.; Szaraz, Z.; D'Agata, E.; Ohms, C.; Martin, O. Influence of Ni-Mn contents on the embrittlement of PWR RPV model steels irradiated to high fluence values relevant for LTO beyond 60 years. *J. Nucl. Mater.* **2021**, *553*, 153036. [CrossRef]
18. Martin, O.; Brumovsky, M.; Kryukov, A. Technical Report: Origin and Manufacturing of the LYRA-10 Specimens. STRUMAT-LTO Report. 2021.
19. ASTM. *Standard Test Methods for Tension Testing of Metallic Materials*; ASTM International: West Conshohocken, PA, USA, 2016.
20. Yabuuchi, K.; Saito, M.; Kasada, R.; Kimura, A. Neutron irradiation hardening and microstructure changes in Fe–Mn binary alloys. *J. Nucl. Mater.* **2011**, *414*, 498–502. [CrossRef]
21. Gillemot, F. Review on Steel Enhancement for Nuclear RPVs. *Metals* **2021**, *11*, 2008. [CrossRef]
22. Gurovich, B.; Kuleshova, E.; Shtrombakh, Y.; Fedotova, S.; Zabusov, O.; Prikhodko, K.; Zhurko, D. Evolution of weld metals nanostructure and properties under irradiation and recovery annealing of VVER-type reactors. *J. Nucl. Mater.* **2013**, *434*, 72–84. [CrossRef]
23. Miller, M.; Chernobaeva, A.; Shtrombakh, Y.; Russell, K.; Nanstad, R.; Erak, D.; Zabusov, O. Evolution of the nanostructure of VVER-1000 RPV materials under neutron irradiation and post irradiation annealing. *J. Nucl. Mater.* **2009**, *385*, 615–622. [CrossRef]
24. Happy, R.N.; Becquart, C.; Domain, C.; Malerba, L. Formation and evolution of MnNi clusters in neutron irradiated dilute Fe alloys modelled by a first principle-based AKMC method. *J. Nucl. Mater.* **2012**, *426*, 198–207. [CrossRef]
25. Kryukov, A.M.; Nikolaev, Y.A.; Nikoleava, A.V. Behavior of mechanical properties of nickel-alloyed reactor pressure vessel steel under neutron irradiation and post-irradiation annealing. *Nucl. Eng. Des.* **1998**, *186*, 353–359. [CrossRef]